Virologica Sinica 38 (2023) 931–939

Contents lists available at ScienceDirect

Virologica Sinica

journal homepage: www.keaipublishing.com/en/journals/virologica-sinica
www.virosin.org

Research Article

Allopregnanolone targets nucleoprotein as a novel influenza virus inhibitor

Meiyue Dong [a,1], Yanyan Wang [b,1], Ping Li [b], Zinuo Chen [a], Varada Anirudhan [c], Qinghua Cui [a,d,*], Lijun Rong [c,*], Ruikun Du [a,d,*]

[a] Innovative Institute of Chinese Medicine and Pharmacy, Shandong University of Traditional Chinese Medicine, Jinan, 250355, China
[b] College of Pharmacy, Shandong University of Traditional Chinese Medicine, Jinan, 250355, China
[c] Department of Microbiology and Immunology, College of Medicine, University of Illinois at Chicago, Chicago, 60612, USA
[d] Qingdao Academy of Chinese Medical Sciences, Shandong University of Traditional Chinese Medicine, Qingdao, 266122, China

ARTICLE INFO

Keywords:
Allopregnanolone (ALLO)
Antiviral
Influenza A virus (IAV)
Nucleoprotein
Nucleus translocation

ABSTRACT

Influenza A virus (IAV) poses a global public health concern and remains an imminent threat to human health. Emerging antiviral resistance to the currently approved influenza drugs emphasizes the urgent need for new therapeutic entities against IAV. Allopregnanolone (ALLO) is a natural product that has been approved as an antidepressant drug. In the present study, we repurposed ALLO as a novel inhibitor against IAVs. Mechanistic studies demonstrated that ALLO inhibited virus replication by interfering with the nucleus translocation of viral nucleoprotein (NP). In addition, ALLO showed significant synergistic activity with compound 16, a hemagglutinin inhibitor of IAVs. In summary, we have identified ALLO as a novel influenza virus inhibitor targeting NP, providing a promising candidate that deserves further investigation as a useful anti-influenza strategy in the future.

1. Introduction

Influenza A virus (IAV) is a major cause of morbidity and mortality from epidemic and pandemic influenza infections, which is a serious global public health threat (Taubenberger and Kash, 2010). Currently, two main strategies are being used to control IAV infections: vaccination and antiviral treatment. Although vaccination is the principal prophylactic methodology for preventing influenza infections (Das et al., 2010; Tscherne and Garcia-Sastre, 2011), its efficacy is highly dependent on the accurate forecast of the circulating strains and also, it is limited in the occurrence of a pandemic (Poland, 2010). There are three classes of anti-influenza agents currently available worldwide, including the viral ion channel M2 blockers (amantadine and rimantadine) (Li et al., 2015; Jalily et al., 2020), the neuraminidase (NA) inhibitors (oseltamivir, zanamivir and peramivir) (Alame et al., 2016), and the RNA-dependent RNA polymerase (RdRp) inhibitors (favipiravir and baloxavir marboxil) (Noshi et al., 2018; Shiraki and Daikoku, 2020). However, almost all circulating influenza strains showcase resistance to M2 inhibitors, and therefore, they are no longer recommended for clinical use (van der Vries et al., 2013). In addition, the incidence of increasing resistance to NA and RdRp inhibitors also impedes their respective efficacies (Goldhill et al., 2018; Hayden et al., 2018; Lackenby et al., 2018; Takashita et al., 2019). Overall, there is an increasing requirement to develop new classes of influenza antiviral agents that target viral proteins involved in virus replication to treat influenza virus infection.

The viral nucleoprotein (NP) is a critical protein at many stages during the influenza viral life cycle. Primarily, the viral genomic RNAs are coated with multiple copies of NP to form the viral ribonucleoprotein (vRNP) complexes (Arranz et al., 2012). Thus, the translocation of NP between the cytoplasm and the nucleus is critical during viral transcription and replication (Newcomb et al., 2009; Turrell et al., 2013), nuclear import/export of the vRNPs (Kao et al., 2010; Chutiwitoonchai et al., 2014) and virion assembly (Noton et al., 2007). Considering these factors, the IAV NP has become one of the most attractive targets for new antiviral development (Hu et al., 2017), and several NP inhibitors including FA6005 (Yang et al., 2021), S119 (White et al., 2018), naproxen (Zheng et al., 2019), RK424 (Kakisaka et al., 2015), Amaryllidaceae alkaloid (He et al., 2013), PPQ581 (Lin et al., 2015), KPT335 (Perwitasari et al., 2014), KR23502 (Jang et al., 2016), H7 (Liu et al., 2016), and 3-mercapto-1,2,4-triazole (Liu et al., 2016) have been reported in the past ten years. Moreover, since NP is a multifunctional viral protein, most of the amino acid residues play essential roles in the viral

* Corresponding authors.
E-mail addresses: cuiqinghua@sdutcm.edu.cn (Q. Cui), lijun@uic.edu (L. Rong), ruikun@sdutcm.edu.cn (R. Du).
[1] Meiyue Dong and Yanyan Wang contributed equally to this work.

https://doi.org/10.1016/j.virs.2023.09.003
Received 11 June 2023; Accepted 19 September 2023
Available online 22 September 2023

life cycle. As a result, a proportion of currently identified inhibitors that recognize the highly conserved pockets of NP are less prone to induce resistance. For instance, passaging IAVs in presence of KR-23502 for 17 rounds generates a slight resistance with only 2-fold increase in median effect dose (EC_{50}) (Jang et al., 2016), while no escape mutant was generated with the virus passaging under the selective pressure of RK424 or NUD-1 (Kakisaka et al., 2015; Makau et al., 2020). The high barrier to drug resistance further highlights the value of NP as a target for novel antiviral development.

Allopregnanolone (ALLO) is a 3α,5α-metabolite of progesterone, and acts as a potent allosteric modulator of the γ-aminobutyric acid type A receptor ($GABA_A$). Decreased levels of ALLO are usually related to mood disorders, such as anxiety-like behavior and depression, post-partum depression and post-partum anxiety (Diviccaro et al., 2022). So far, ALLO (brexanolone) has been developed and approved by the FDA for the treatment of postpartum depression (Edinoff et al., 2021). Previously, we had performed a phenotypic antiviral screen of 891 natural products using a reporter influenza PR8-PB2-Gluc virus for novel anti-influenza activities and identified ALLO as one of the most potent hits (Zhao et al., 2019). In this study, we further validated the anti-influenza activity of ALLO, and investigated its mechanism of action by targeting viral NP protein.

2. Materials and methods

2.1. Cell culture and viruses

Human embryonic kidney 293T cells (GNHu17) and canine kidney epithelial MDCK cells (GNO23) were obtained from the Cell Bank/Stem Cell Bank, Chinese Academy of Sciences (Shanghai, China), and grown in Dulbecco's modified Eagle's medium (DMEM; Cellgro, Manassas, VA, USA) supplemented with 10% fetal bovine serum (FBS; Gibco, Carlsbad, CA, USA), 1000 units/mL penicillin, and 100 μg/mL streptomycin (Invitrogen, Carlsbad, CA, USA). During virus experiments, MDCK cells were maintained in Opti-MEM containing 1.5 μg/mL N-tosyl-L-phenylalanine chloromethyl ketone (TPCK)-trypsin (Sigma-Aldrich, St. Louis, MO, USA). All cells were grown at 37 °C in 5% CO_2 incubator.

Influenza A/Puerto Rico/8/1934 virus (A/PR8, H1N1), recombinant influenza A reporter viruses PR8-PB2-Gluc and PR8-Fluc were prepared and stored in our lab as previously described (Zhao et al., 2018, 2022). Influenza A/Brisbane/10/2007 (A/Brisbane, H3N2) was provided by Chinese Academy of Medical Sciences, and influenza B/Phuket/3073/2013-Yamagata and B/Brisbane/60/2008-Victoria viruses were provided by Shandong center for disease control and prevention (Jinan, China).

2.2. Dose–response assay

For dose–response analysis, cells grown in white 96-well plates were inoculated with influenza A/PR8-PB2-GLuc (MOI = 0.01). After 1 h incubation, the inoculum was replaced with Opti-MEM (2 μg/mL TPCK-trypsin) containing increasing concentrations of tested compound. At around 36 h post infection (h.p.i.), *Gaussia* luciferase activity was measured by using Pierce *Gaussia* luciferase Glow Assay kit (Thermo Scientific, USA) following the manufacturer's instruction. Cell viability was examined with CCK-8 (MCE, USA) according to manufacturer's protocol. The 50% inhibiting concentration (IC_{50}) and 50% cytotoxic concentration (CC_{50}) values were determined by fitting dose–response curves with a four-parameter logistic regression to the data in GraphPad Prism software (version 5.02, La Jolla, CA, United States).

2.3. Viral titer reduction assay

MDCK cells growing in 24-well plates were infected with the A/PR8, A/Brisbane, B/Yamagata, and B/Victoria strains at MOI of 0.01. After 2 h of incubation, the cells were cultured with Opti-MEM containing 1.5 μg/mL of TPCK-trypsin as well as DMSO or various concentrations of ALLO. The plates were incubated at 37 °C and culture supernatants were collected at 36 h.p.i., and virus titers [median tissue culture infective dose ($TCID_{50}$)/mL] in the culture supernatants were determined.

2.4. Animal experiments

Female BALB/c mice (4–6 weeks old) were purchased from Charles River Laboratory Animal Technology (Beijing, China) and maintained under specific pathogen-free conditions. All efforts were made to minimize any suffering and the number of animals.

For mouse infections, mice were intranasally inoculated under isoflurane anesthesia with the recombinant influenza PR8-Fluc virus at a dose of 1000 $TCID_{50}$. At day 2 p.i., bioluminescence imaging was performed as previously described (Lin et al., 2023). In brief, mice were anaesthetized and intraperitoneally administered with the substrate D-luciferin at 150 mg/kg, and then subjected to image acquisition using the Xenogen IVIS 200 (PerkinElmer, Waltham, USA) after 10 min. The images were analyzed using the Living Image software (version 4.4).

For antiviral determination, groups of mice (n = 3) were separately treated with ALLO (40 mg/kg/day), the vehicle only (PBS) as negative control, and oseltamivir phosphate (30 mg/kg/day) as positive control. All treatment was given intraperitoneally twice a day, starting at 2 h before virus inoculation.

2.5. Time-of-addition assay (TOA)

A total of 1×10^5 MDCK cells per well were cultured in 24-well plates 1 day prior to the assay. Then, cells were infected with 0.1 MOI of A/H1N1/PR8 virus at 4 °C for 1 h, and then transferred to 37 °C for 1 h. After virus attachment, culture wells were washed with PBS to remove unbound viral particles and incubated at 37 °C. The time point when plates were transferred to 37 °C was set as 0 h.p.i. The cells were treated with the 20 μmol/L ALLO or DMSO at the indicated time intervals (−2 to 12, −2 to 0, 0 to 12, 2 to 12, 4 to 12, 6 to 12, and 8 to 12 h), which cover the first viral replication cycle. After 12 h.p.i., supernatants were collected and viral yields were determined by $TCID_{50}$ assay. Every condition was tested in triplicate.

2.6. Mini-replicon assay

The effect of ALLO on the activity of the vRNP was determined by using a mini-genome assay in 293T cells as previously described (Jang et al., 2016). In brief, 293T cells grown in 6-well plates were transfected with plasmids (pCAG-VN04-NP, pCAG-VN04-PA, pCAG-VN04-PB1, pCAG-VN04-PB2), the minigene plasmid pPolI-NS-Fluc and a control plasmid pRL-TK using Lipofectamine 2000 (Invitrogen) according to the manufacturer's manual. At 5 h after transfection, the transfected cells were seeded into white, flat-bottom, 96-well plates at a density of 1×10^5 cells/well in a 100 μL assay medium, containing DMSO or various concentrations of ALLO. At 24 h post-transfection, luciferase activity was measured by using dual-luciferase reporter assay system (Promega, Madison, WI, USA) according to the manufacturer's manual.

2.7. Immunofluorescence (IF) microscopy

MDCK cells were grown to 70%–80% confluency on 24-well glass bottom plate, followed by infecting with A/PR8 virus for 2 h at MOI = 5 in the presence or absence of 40 μmol/L ALLO and washed. ALLO or DMSO were maintained in culture throughout the experiment. Infections were stopped at indicated time points by fixation in 4% paraformaldehyde for 30 min at room temperature. After fixation, the cells were washed with PBS three times and permeabilized with 0.5% Triton-X100 for 15 min, then blocked with 5% BSA for 30 min. Subsequently, cells were incubated for 1 h with primary antibodies against NP (Gene Tex, USA; product number: GTX125989) in 1% BSA (dilution 1:500),

followed by staining with CoraLite 488-conjugated goat secondary antibody against rabbit IgG (H + L) (Proteintech, USA) in 1% BSA (dilution 1:500) for 1 h. Cells were then washed and counterstained with 4′,6-diamidino-2-phenylindole, dihydrochloride (DAPI) for nucleus localization before image analysis by LSM880 confocal microscope (Zeiss, Germany).

2.8. Thermal shift assay

To perform the thermal shift assay, 30 μL of solution containing 10 μmol/L recombinant NP protein of influenza A/PR8/Mount Sinai (Sino Biological, China) was mixed with 10 μL of 5× SYPRO Orange dye (MERCK, Germany) and 10 μL of ALLO (1.6 mmol/L) or DMSO as a negative control. The mixture was then subjected to a CFX Real-Time PCR Detection System (Bio-Rad, USA). The temperature was set from 25 °C to 90 °C at a rate of 1 °C min^{-1} and the fluorescence changes were monitored every minute.

2.9. Molecular docking of ALLO to NP

To predict the binding mode of ALLO to NP, molecular docking simulations was conducted using the AutoDock 4.2 software (The Scripps Research Institute, USA) (Morris et al., 2009). The crystal structure of NP protein from influenza A/H1N1/PR8 (PDB ID: 2IQH) was used, and the 3-dimensional structure of ALLO was generated by Chem3D (CambridgeSoft, USA).

Before docking simulation, the NP structure was pre-processed by removing water molecules and adding hydrogen atoms using the AutoDock tools. Docking was performed using a grid box of 126 Å in size and grid-point spacing of 0.436 Å. Subsequent analysis of the interaction between ALLO and NP was conducted using a molecular visualization tool PyMOL (Version 1.8, Schrodinger, Seattle, USA) to generate the surfaces of NP to help spotting the binding sites of ALLO on the interfaces of NP.

2.10. Synergistic studies

MDCK cells were seeded into white, flat-bottom, 96-well culture plates (PerkinElmer) at a density of 1×10^4 cells/well 24 h prior to infection. Cells were then infected with recombinant reporter virus PR8-PB2-Gluc at an MOI of 0.01 and treated with varying doses of ALLO alone, compound 16 alone (Gaisina et al., 2020), or ALLO and compound 16 in combination. After 36 h incubation, infection was determined through the *Gaussia* luciferase activity using Pierce *Gaussia* Luciferase Glow Assay kit (Thermo Fisher, Hillsboro, OR, United States). The IC_{30}, IC_{40}, IC_{50}, IC_{60}, IC_{70}, and IC_{80} values were chosen for comparison. Combination index (CI) values were calculated using the CompuSyn software (Biosoft, Ferguson, USA) (Chou, 2010). The combination effect was determined based on the following criteria: CI < 1.0, synergy; CI = 1.0, additive; CI > 1.0, antagonism.

3. Results

3.1. Identification of ALLO as a novel inhibitor of IAV

With the goal to discover novel influenza virus inhibitors, we had previously developed a phenotypic screening approach using a reporter IAV expressing *Gaussia* luciferase (PR8-PB2-Gluc), and we had then carried out a primary screen of a library consisting of 891 natural products (Zhao et al., 2019; Kang et al., 2020). In this study, we focused on one of the most potent hits, ALLO (Fig. 1A), for its anti-influenza potency. As shown in Fig. 1B, ALLO exhibited reasonable antiviral activity against PR8-PB2-Gluc virus, with an IC_{50} value of 6.27 μmol/L and a CC_{50} value of >100 μmol/L, generating a selectivity index (SI) higher than 15.9. As a positive control, oseltamivir acid was validated for its anti-IAV activity using the PR8-PB2-Gluc virus in parallel.

To further evaluate the antiviral activity of ALLO against influenza viruses, a titer reduction assay was performed using a variety of wildtype IAV strains as well as influenza B viruses (IBVs). As shown in Fig. 1C, ALLO showed inhibitory effects in a dose-dependent manner against IAV strains, including A/PR8 and A/Brisbane, which represent subtype H1N1 and H3N2 respectively. However, both IBV strains Yamagata and Victoria showed less sensitivity to ALLO compared to IAVs, since the propagation of IBVs were inhibited by ALLO at higher concentrations. Moreover, neither the B/Yamagata nor B/Victoria strains could be completely inhibited at as high as 40 μmol/L, at which concentration the IAVs produced no detectable progeny virions (Fig. 1C). As a positive control, the active metabolite of baloxavir marboxil (baloxavir acid) showed significant inhibitory effects against the virus yield of both IAV and IBV strains (Fig. 1D).

Moreover, we have also preliminarily tested the antiviral potency of ALLO using a bioluminescence imaging (BLI)-based mouse model of IAV infection, and it turned out that although without statistical significance ($P = 0.08$), reduced tendency of virus replication *in vivo* was observed after ALLO treatment (Fig. 1E and F). Together, these results indicate that ALLO is a novel potent inhibitor against IAVs, although it also shows some extent of inhibition against IBVs.

3.2. ALLO interferes with the late stages of viral life cycle

To investigate the mechanism of action of ALLO upon IAV replication, a TOA assay was conducted. Briefly, the influenza PR8 virus (0.1 MOI) was inoculated to MDCK cells at 4 °C for 1 h followed by transferring to 37 °C for another 1 h to allow synchronized infection. Then the inoculum was replaced by fresh medium for further incubation; this time point was set as 0 h. ALLO was added at an interval of 2 h starting from −2 h, while ALLO treatment between −2 to 0 h only was performed to exclude the possibility that ALLO acted against virus entry (Fig. 2A). As shown in Fig. 2B, adding ALLO at a time point as late as 4 h.p.i. resulted in complete inhibition, whereas treatment starting at 6 h or later markedly alleviated the inhibitory effects. As a control, oseltamivir acid, which blocks the release of progeny virions from infected cells, can significantly decrease the virus yield when added at a very late interval of 8 to 12 h.p.i. Together, these results suggest that ALLO acts against the late stages of influenza virus life cycle.

Since the viral genome replication is a key process that occurs at the late stage of the viral life cycle, we next evaluated the effect of ALLO on viral genome replication using a cell-based influenza RdRp assay. As a result, it was demonstrated that ALLO significantly blocked viral RdRp activity in a dose-dependent manner (Fig. 2C). This result suggests that ALLO may act by targeting directly to the vRNP complex, or host factors that are involved in IAV RNA transcription/replication processes (Wang et al., 2015; Zhang et al., 2023).

3.3. ALLO interferes with the nucleus translocation of vRNP

The shuttling of influenza vRNP between cytoplasm and nucleus plays an essential role during viral genome replication, and thus, blocking vRNP nuclear transport impairs the activity of vRNP complex (Zhang et al., 2016). We herein asked whether ALLO affects the nuclear transport of vRNP. To address this, MDCK cells were infected with IAVs followed by treatment with ALLO or DMSO (as a negative control). The translocation of NP was monitored at different time points after infection using an IF assay. Considering NP proteins are the major components of the influenza vRNP complex, the location of NP can represent the location of vRNP complex in the infected cells.

As shown in Fig. 3, the NPs in the form of incoming vRNPs were localized in the cytoplasm of both DMSO and ALLO treated cells at 0 h.p.i., suggesting successful internalization of infecting virions, which is consistent with the above results from the TOA assay that ALLO treatment between −2 to 0 h did not affect virus entry. However, it was

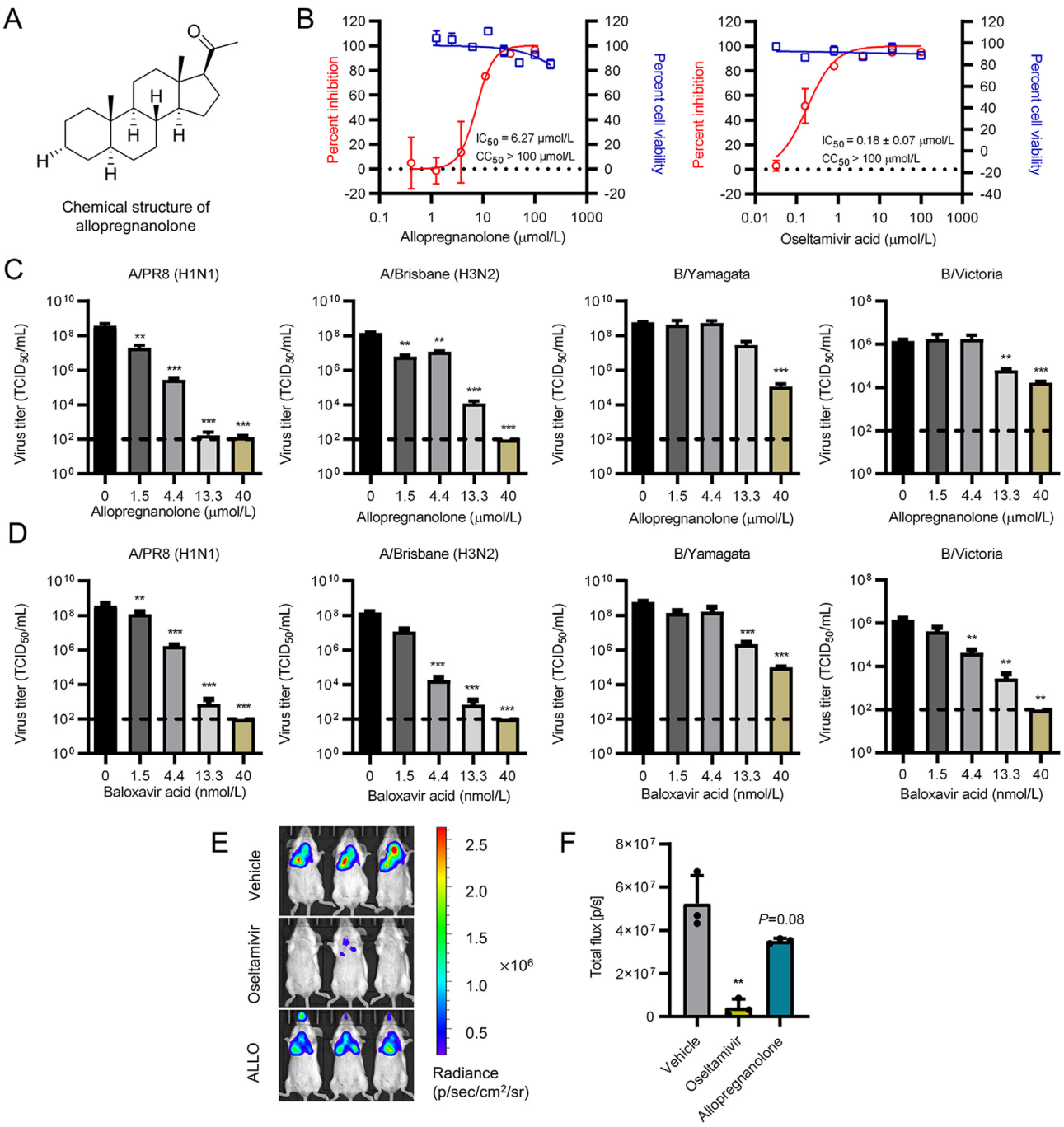

Fig. 1. Antiviral determination of allopregnanolone (ALLO) against influenza viruses. **A** The chemical structure of compound ALLO. **B** The dose–response effect of ALLO and oseltamivir acid upon PR8-PB2-Gluc virus replication and viabilities of MDCK cell. MDCK cell were infected with reporter influenza PR8-PB2-Gluc virus at an MOI of 0.01 in the presence of serial concentrations of ALLO. At 48 h post infection (h.p.i.), luciferase assay was performed to monitor virus replication. The IC_{50} and CC_{50} values were calculated using GraphPad Prism 5. **C**, **D** Viral titer reduction assay. MDCK cells were infected with wildtype Influenza A/PR8 (H1N1), A/Brisbane (H3N2), B/Yamagata and B/Victoria viruses at an MOI of 0.01 and treated with indicated concentrations of ALLO (**C**) and baloxivir acid (**D**) separately. At 36 h.p.i., the virus yields ($TCID_{50}$/mL) were determined. Dashed lines indicate the limit of detection. Values were expressed as means ± SEM (n = 3). $^{**}P < 0.01$; $^{***}P < 0.001$; student's *t*-test. **E**, **F** *In vivo* antiviral evaluation. Female BALB/c mice (4–6 weeks old) were intranasally inoculated with recombinant influenza PR8-Fluc virus at a dose of 1000 $TCID_{50}$, and received treatment with ALLO at 40 mg/kg/day twice daily, starting at 2 h before virus infection. Mice treated with vehicle only (PBS) and oseltamivir phosphate (30 mg/kg/day) were set as negative and positive control respectively. At day 2 p.i., bioluminescence imaging was performed (**E**) and the signal densities were analyzed (**F**). Values were expressed as means ± SEM (n = 3). $^{**}P < 0.01$, student's *t*-test.

observed that the nuclear import of incoming vRNPs was greatly delayed from 2 h.p.i. to 4 h.p.i. by ALLO (Fig. 3A and B). Moreover, in the cells treated with DMSO as negative control, the NPs were predominantly located in the cytoplasm at 8 h.p.i., while in ALLO treated cells most NP proteins were located in the nucleus (Fig. 3A and B). These results demonstrated that in the presence of ALLO, the newly synthesized NP proteins were able to enter the nucleus, however, their export later in to the cytoplasm in the form of vRNP was drastically impaired. Additionally, it is noteworthy that the newly synthesized NPs ALLO treated cells were detected as discrete spots instead of disperse distribution in the nucleus, suggesting the formation of abnormal NP aggregates (Fig. 3B, Supplementary Fig. S1).

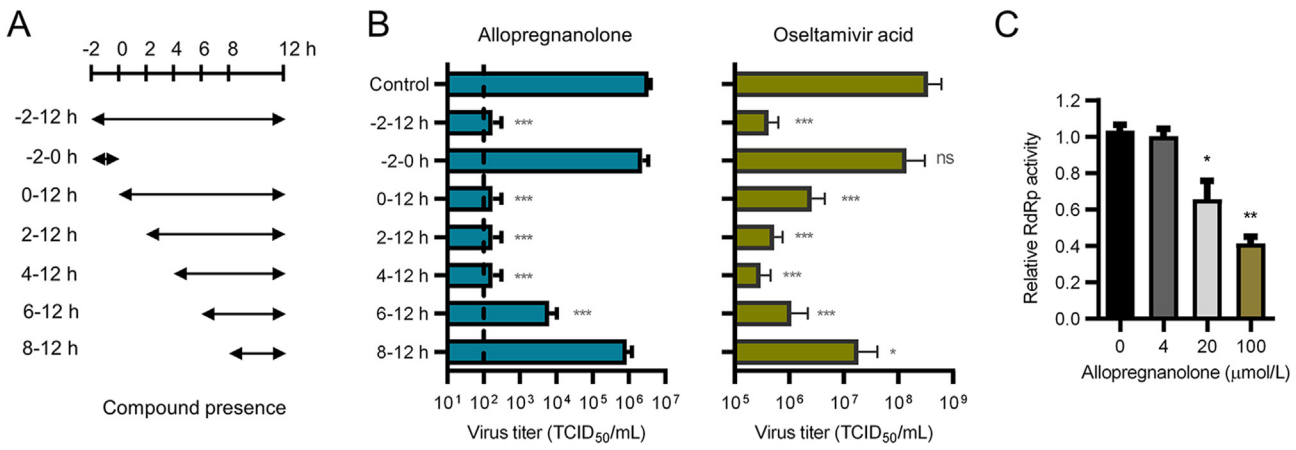

Fig. 2. Mechanistic studies for the antiviral effect of allopregnanolone (ALLO) against influenza viruses. **A** Schematic presentation of the time-of-addition assay. **B** Time-of-addition assay. MDCK cells were infected with influenza A/PR8 virus at an MOI of 0.01 and treated with ALLO or oseltamivir acid at indicated time intervals. The virus yields ($TCID_{50}$/mL) were determined at 12 h post infection. **C** Cell-based RNA-dependent RNA polymerase (RdRp) assay. The inhibitory effect of ALLO on viral RdRp activity was tested using a mini-replicon based RdRp assay in 293T cells. Values were expressed as means ± SEM (n = 3). $^{*}P < 0.05$; $^{**}P < 0.01$; $^{***}P < 0.001$; student's *t*-test.

3.4. ALLO acts by directly binding to NP

Taking into consideration that ALLO treatment induces NP aggregation and retention in the nucleus, we speculated that ALLO may act by directly binding to NP. To confirm this, a thermal shift assay was performed. Briefly, 10 μmol/L of recombinant IAV NP protein was incubated with 1.6 mmol/L ALLO and 5× SYPRO Orange dye, followed by fluorescence scanning as the temperature raised gradually. As shown in Fig. 4A, the melting temperature (Tm) of NP in absence or presence of ALLO is 43.91 and 39.37 °C, respectively, generating a shift (ΔTm) of −4.54 ± 0.13 °C. This result clearly demonstrates that ALLO binds directly to NP, destabilizing the target protein.

To better deduce the binding mode of ALLO with IAV NP, an *in silico* docking analysis was performed to evaluate the potent affinity between ALLO and the published crystal structure of influenza A/PR8 (H1N1) NP trimer. As a result, five potential sites within NP for ALLO binding were

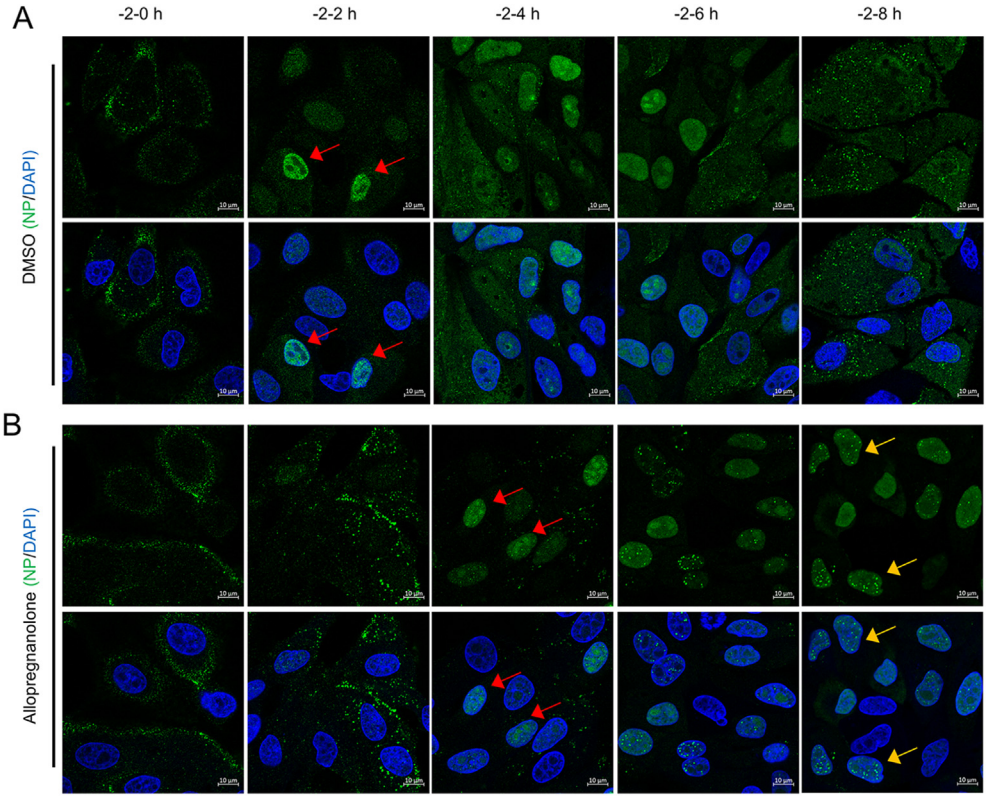

Fig. 3. The subcellular localization of nucleoprotein (NP) during IAV infection in absence or presence of allopregnanolone (ALLO). The MDCK cells were infected with influenza A/PR8 virus and treated with **(A)** DMSO or **(B)** ALLO (40 μmol/L). At indicated time points, cells were fixed and stained with an anti-NP antibody (green). The nucleus was stained with DAPI (blue). The nuclear import of incoming vRNPs were indicated by red arrows, while the abnormal aggregation of newly synthesized NPs within the nucleus was indicated by yellow arrows. Scale bar = 10 μm.

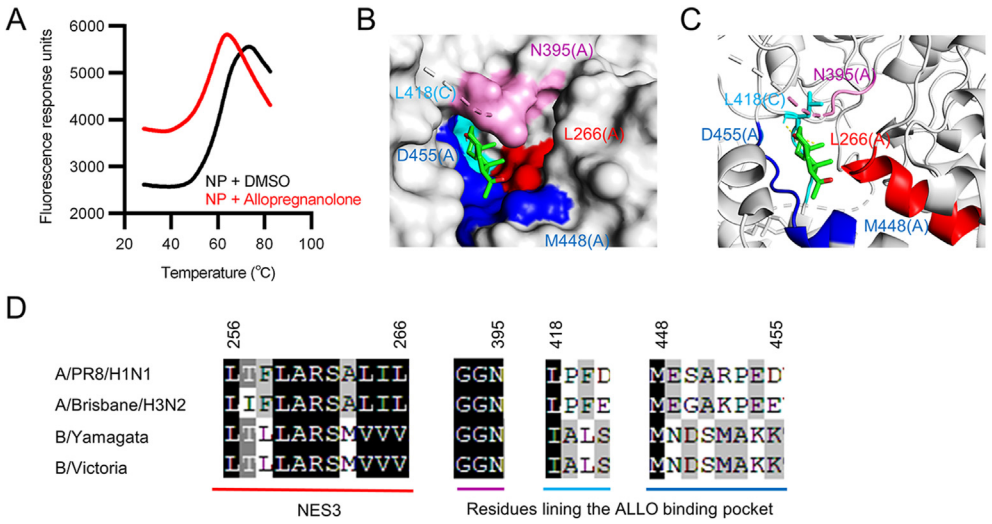

Fig. 4. Binding mode of allopregnanolone (ALLO) to nucleoprotein (NP). **A** Thermal shift assay. The thermal stability of recombinant IAV NP protein was determined in absence or presence of ALLO. The data shown are representative of three independent experiments. **B, C** The binding of ALLO to NP (PDB ID: 2IQH) was predicted by Auto-Dock software, and the configuration of ALLO-NP complex harboring the highest binding free energy were shown in **(B)** surface or **(C)** cartoon. The residues forming the binding pocket were colored in cyan (L418–D421), pink (G393–N395), red (L266) and blue (M448–D455). The amino acids 256–266 representing nuclear export signal 3 (NES3) were shown in red. The brackets indicate the chains of NP trimer. **D** Alignment of ALLO-binding pocket related sequences between ANPs and BNPs.

predicted, with the best fitting one showing a binding free energy (−ΔG) as high as 8 kcal/mol (Supplementary Fig. S2). The configuration with the best binding score is shown in Fig. 4B and C presenting surface and cartoon, respectively. It was demonstrated that ALLO can bind to a pocket in proximity to the residue L266 which represents the C-terminus of the nuclear export signal 3 (NES3, amino acids 256–266), while the residue L418 from adjacent NP monomer played an essential role in ALLO-NP binding by forming hydrogen bonds (Fig. 4C).

The NP proteins are highly conserved among IAVs or IBVs; however, the IAV NP (ANP) and IBV NP (BNP) share limited amino acid sequence homology. The binding mode of ALLO to BNP might be different from that of ALLO-ANP. Since there is no published crystal structure of BNP trimer for *in silico* docking studies, the residues lining the ALLO-binding pocket within ANP were aligned to the corresponding sequences of BNP. As shown in Fig. 4D, the NES3 sequences are conserved between both ANP and BNP, so as the residue N395, which lines in the same side of the ALLO-binding pocket with L266. However, the amino acids 448–455 representing the other side of the ALLO-binding pocket varied between ANP and BNP. In addition, the amino acid residues 418–421 which were located at the bottom of the pocket are variable, leaving only L418 conserved between ANP and BNP. These variations may result in an altered configuration of the related pocket within BNP, and the fitness for ALLO binding might change accordingly.

3.5. ALLO synergizes with an HA inhibitor compound 16

Combining antiviral agents that showcase different mechanisms of actions can significantly preclude the emergence of drug resistance, and moreover, synergistic antiviral effect might be achieved. It is interesting to understand how ALLO interacts with currently approved influenza drugs and those candidates in development. To this end, we tested the antiviral effect of the ALLO in combination with compound 16, a novel HA inhibitor of IAV that we had previously identified (Gaisina et al., 2020). MDCK cells were infected with reporter influenza PR8-PB2-Gluc virus at an MOI of 0.01 and treated with increasing concentrations of ALLO alone, compound 16 alone, or ALLO and compound 16 in combination. In combination assays, a constant concentration (27 nmol/L) of compound 16 was used, corresponding to 20% inhibition concentration for the drug as a single agent. The concentrations of ALLO to cause 30, 40, 50, 60, 70, 80, and 90% reductions in luciferase expressing levels (IC_{30}–IC_{90}) were subsequently determined and the CI values were evaluated by the median effect plot method.

As shown in Table 1, individually administered ALLO was not as effective in preventing the infectivity compared to when it was applied in combination. The lowest value of CI (0.78) was achieved with the treatment with ALLO and compound 16 used at 6.05 μmol/L and 27 nmol/L, respectively, leading to a 50% reduction in viral replication.

Table 1
Synergistic anti-influenza activity of ALLO and compound 16.

Compound	IC_{30} (μmol/L)	IC_{40} (μmol/L)	IC_{50} (μmol/L)	IC_{60} (μmol/L)	IC_{70} (μmol/L)	IC_{80} (μmol/L)
ALLO	3.49	4.65	6.05	7.87	10.49	14.88
Compound 16	0.032	0.039	0.046	0.055	0.066	0.083
ALLO + Compound 16 (27 nmol/L)	0.28	0.60	1.19	2.36	4.99	12.40
CI	0.91	0.82	0.78	0.79	0.88	1.16

CI, combination index.

These results suggest that ALLO may act in synergy with compound 16 against IAV infection.

4. Discussion

In this study, we repurposed ALLO as a novel antiviral agent against influenza viruses, including both IAVs and IBVs. Further mechanistic studies demonstrates that ALLO prevents influenza virus replication by targeting NP mainly through multi-modes of action (Fig. 5). First, ALLO treatment delays the nucleus import of NPs in the form of incoming vRNPs; second, ALLO treatment prevents the nucleus export of NPs in the form of newly synthesized vRNPs; third, ALLO treatment induces higher-order oligomerization of the NP proteins, interfering with the formation of new cRNPs and vRNPs.

Upon entry into the host cells, the infectious influenza virions release the genetic components, i.e., vRNPs, into the cytoplasm. Next, the incoming vRNPs enter the nucleus to initiate genome transcription and subsequent replication (Du et al., 2022). Dissociation of vRNPs from M1 is a prerequisite for vRNP translocation into the nucleus as it exposes the nuclear localization signals (NLS) (Martin and Helenius, 1991). Previously, Yang et al. had reported that FA6005, an NP inhibitor of IAV, can perturb the trafficking of vRNPs at early stages by preventing M1-vRNP dissociation (Yang et al., 2021). Interestingly, our results also indicated that ALLO treatment delayed the translocation of incoming vRNPs into nucleus, implying that ALLO binding to NP may reduce the efficiency of M1-vRNP dissociation during the virus uncoating process (Fig. 3).

After translocation into the host nucleus, the transcription of viral RNA (vRNA) is initiated and viral messenger RNAs (mRNA) are then released to the cytoplasm, where viral proteins are translated. The newly synthesized NP and RdRp constituents (PA, PB1 and PB2) are subsequently translocated into the nucleus, followed by vRNA replication and formation of progeny vRNPs. Eventually, these progeny vRNPs are exported to the cytoplasm for virion assembly and budding (Du et al., 2022). Notably, our results have demonstrated that ALLO treatment interfered with the nuclear export of NP, thus blocking propagation of progeny virions (Fig. 3). The NP protein contains three NES sequences (NES1, NES2 and NES3) that play critical roles during vRNP export from the nucleus (Yu et al., 2012). Interestingly, an *in silico* docking study predicted that ALLO can bind to the NES3 region of NP (Fig. 4B and C), suggesting that ALLO binding may shelter the NES3 thus preventing NP export.

In addition, we observed that ALLO treatment induces abnormal aggregation of NP in the nucleus (Fig. 3B). Generally, the newly synthesized NP monomers in the cytoplasm are imported to the nucleus, where they are involved in the formation of new cRNP/vRNP and nuclear export of progeny vRNPs (Yu et al., 2012). The formation of higher-order NP

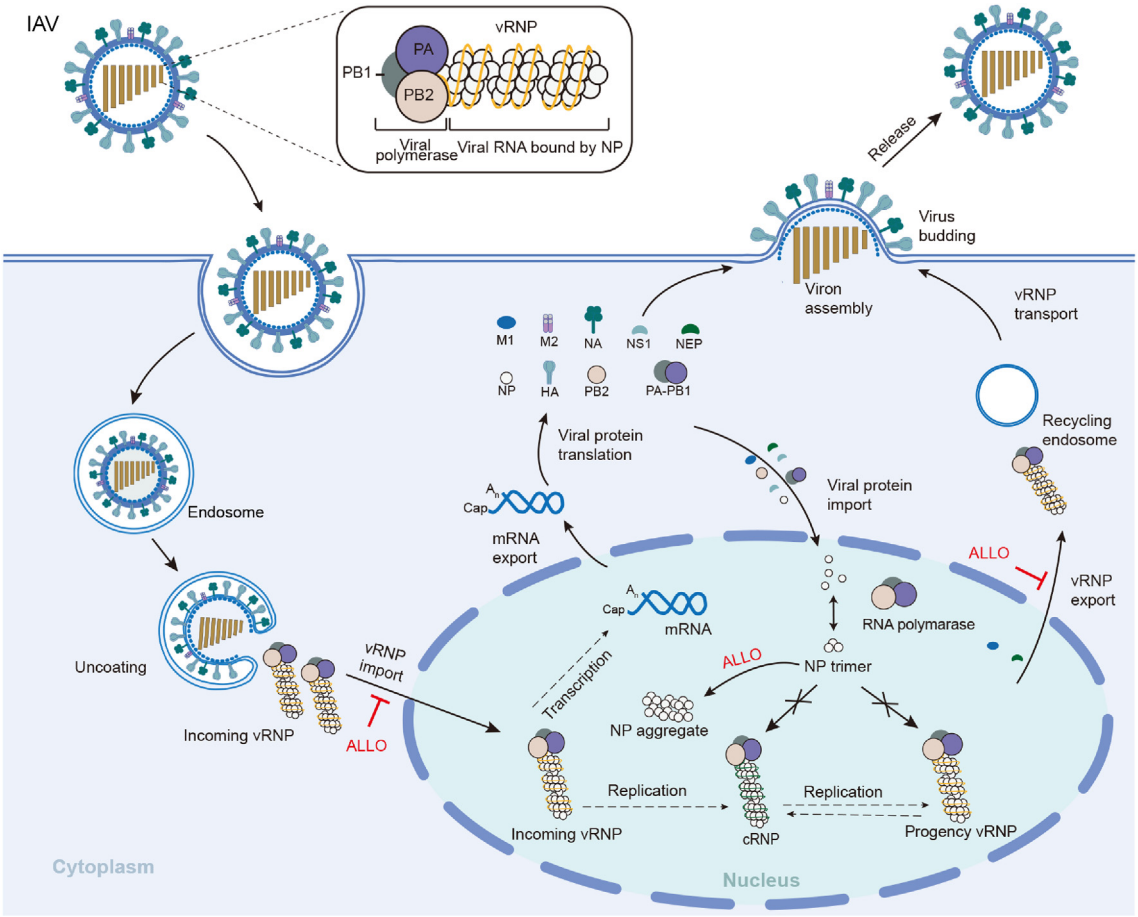

Fig. 5. Schematic representation of the mechanism underlying the anti-influenza effect of allopregnanolone (ALLO). Upon entry into the host cells, the infectious influenza virions release the inner genetic contents, i.e., vRNPs, to the cytoplasm. Next, the incoming vRNPs enter the nucleus to initiate genome transcription. As viral messenger RNAs (mRNA) are then released to the cytoplasm, where viral proteins are translated, and the newly synthesized NP and RdRp constituents (PA, PB1 and PB2) are subsequently translocated into the nucleus, followed by vRNA replication and formation of progeny vRNPs. Eventually, these progeny vRNPs are exported to the cytoplasm for virion assembly and budding. ALLO treatment interferes with viral replication probably by three modes: first, ALLO treatment delayed the nucleus import of NPs in the form of incoming vRNPs, probably by preventing M1-vRNP dissociation; second, ALLO treatment induces higher-order NP oligomerization, thus blocking the formation of new cRNPs/vRNPs; third, ALLO treatment disturbs the nucleus export of NPs in the form of newly synthesized vRNPs, probably by sheltering the nuclear export site 3 (NES3).

oligomers may interfere with new vRNP/cRNP formation, resulting in the cessation of virus replication (Fig. 5). Interestingly, it has been reported that nucleozin, a well-studied IAV NP inhibitor, can also induce the formation of higher-order NP oligomers by simultaneously recognizing the Y289/N309 and R382/R384 (or Y52/Y313) pockets from two NP trimers (Gerritz et al., 2011; Pang et al., 2016). It is likely that ALLO may also serve as a molecular glue to bridge NP proteins together, although the precise binding modes of ALLO induced NP aggregation remain elusive and deserve further investigation in the future.

Regarding the spectrum of NP inhibitors, it is noteworthy that the IBVs show less sensitive to ALLO treatment compared to IAVs. This might due to the low amino acid sequence conservation of about 38% sequence similarity between ANPs and BNPs, although they have similar functions during viral replication (Sherry et al., 2014). In fact, the NP inhibitors are usually either IAV-specific or IBV-specific, with only a few compounds harboring broad-spectrum antiviral activity against both IAVs and IBVs (White et al., 2018; Yang et al., 2021). As *in silico* docking poses ALLO to a pocket in proximity to the NES3 of ANP, and the amino acid residues 448–455 that are located around the predicted binding pocket varies greatly in BNPs (corresponding to amino acids 504–511), we hypothesized that the configuration of the related pocket of BNP is less fit for ALLO recognition, in accordance to the less sensitivity of IBVs to ALLO treatment.

5. Conclusions

In summary, the findings of the present study suggest ALLO as a promising anti-influenza compound which deserves further investigation as a useful strategy against influenza infections. Additionally, as an approved drug, ALLO could be repurposed for anti-influenza treatment much easier than any other candidate drugs that are currently in development.

Data availability

All relevant data are within the paper and its Supplementary Data.

Ethics statement

All animal procedures were performed in accordance with protocols approved by the Institutional Animal Care and Use Committee (IACUC) of Shandong University of Traditional Chinese Medicine (Approval: SDUTCM20230918401).

Author contributions

Meiyue Dong: investigation, methodology, software, visualization; Yanyan Wang: investigation, methodology, software, visualization; Ping Li: formal analysis, investigation; Zinuo Chen: formal analysis, investigation; Varada Anirudhan: writing - review & editing; Qinghua Cui: data curation, formal analysis, funding acquisition, project administration; Lijun Rong: conceptualization, supervision, writing - review & editing; Ruikun Du: conceptualization, data curation, funding acquisition, supervision, writing - original draft.

Conflict of interest

Prof. Lijun Rong is an editorial board member for *Virologica Sinica* and was not involved in the editorial review or the decision to publish this article. The authors declare no conflict of interest.

Acknowledgments

This study was supported by the National Natural Science Foundation of China (No. 82104134); the Natural Science Foundation of Shandong Province, China (No. ZR2020MH383); the Major Basic Program of Natural Science Foundation of Shandong Province (No. ZR2021ZD17); the Jinan Independent Training Innovative Team (No. 2021GXRC028) and the Open Research Fund Program of the State Key Laboratory of Virology of China (No. 2022IOV003).

Appendix A. Supplementary data

Supplementary data to this article can be found online at https://doi.org/10.1016/j.virs.2023.09.003.

References

Alame, M.M., Massaad, E., Zaraket, H., 2016. Peramivir: A novel intravenous neuraminidase inhibitor for treatment of acute influenza infections. Front. Microbiol. 7, 450.

Arranz, R., Coloma, R., Chichón, F.J., Conesa, J.J., Carrascosa, J.L., Valpuesta, J.M., Ortín, J., Martín-Benito, J., 2012. The structure of native influenza virion ribonucleoproteins. Science 338, 1634–1637.

Chou, T.C., 2010. Drug combination studies and their synergy quantification using the Chou-Talalay method. Cancer Res. 70, 440–446.

Chutiwitoonchai, N., Kakisaka, M., Yamada, K., Aida, Y., 2014. Comparative analysis of seven viral nuclear export signals (NESs) reveals the crucial role of nuclear export mediated by the third NES consensus sequence of nucleoprotein (NP) in influenza A virus replication. PLoS One 9, e105081.

Das, K., Aramini, J.M., Ma, L.C., Krug, R.M., Arnold, E., 2010. Structures of influenza A proteins and insights into antiviral drug targets. Nat. Struct. Mol. Biol. 17, 530–538.

Diviccaro, S., Cioffi, L., Falvo, E., Giatti, S., Melcangi, R.C., 2022. Allopregnanolone: an overview on its synthesis and effects. J. Neuroendocrinol. 34, e12996.

Du, R., Cui, Q., Chen, Z., Zhao, X., Lin, X., Rong, L., 2022. Revisiting influenza A virus life cycle from a perspective of genome balance. Virol. Sin. 38, 1–8.

Edinoff, A.N., Odisho, A.S., Lewis, K., Kaskas, A., Hunt, G., Cornett, E.M., Kaye, A.D., Kaye, A., Morgan, J., Barrilleaux, P.S., Lewis, D., Viswanath, O., Urits, I., 2021. Brexanolone, a GABA(A) modulator, in the treatment of postpartum depression in adults: a comprehensive review. Front. Psychiatry 12, 699740.

Gaisina, I.N., Peet, N.P., Cheng, H., Li, P., Du, R., Cui, Q., Furlong, K., Manicassamy, B., Caffrey, M., Thatcher, G.R.J., Rong, L., 2020. Optimization of 4-aminopiperidines as inhibitors of influenza A viral entry that are synergistic with oseltamivir. J. Med. Chem. 63, 3120–3130.

Gerritz, S.W., Cianci, C., Kim, S., Pearce, B.C., Deminie, C., Discotto, L., McAuliffe, B., Minassian, B.F., Shi, S., Zhu, S., Zhai, W., Pendri, A., Li, G., Poss, M.A., Edavettal, S., McDonnell, P.A., Lewis, H.A., Maskos, K., Mörtl, M., Kiefersauer, R., Steinbacher, S., Baldwin, E.T., Metzler, W., Bryson, J., Healy, M.D., Philip, T., Zoeckler, M., Schartman, R., Sinz, M., Leyva-Grado, V.H., Hoffmann, H.H., Langley, D.R., Meanwell, N.A., Krystal, M., 2011. Inhibition of influenza virus replication via small molecules that induce the formation of higher-order nucleoprotein oligomers. Proc. Natl. Acad. Sci. U. S. A. 108, 15366–15371.

Goldhill, D.H., Te Velthuis, A.J.W., Fletcher, R.A., Langat, P., Zambon, M., Lackenby, A., Barclay, W.S., 2018. The mechanism of resistance to favipiravir in influenza. Proc. Natl. Acad. Sci. U. S. A. 115, 11613–11618.

Hayden, F.G., Sugaya, N., Hirotsu, N., Lee, N., de Jong, M.D., Hurt, A.C., Ishida, T., Sekino, H., Yamada, K., Portsmouth, S., Kawaguchi, K., Shishido, T., Arai, M., Tsuchiya, K., Uehara, T., Watanabe, A., Baloxavir Marboxil Investigators Group, 2018. Baloxavir marboxil for uncomplicated influenza in adults and adolescents. N. Engl. J. Med. 379, 913–923.

He, J., Qi, W.B., Wang, L., Tian, J., Jiao, P.R., Liu, G.Q., Ye, W.C., Liao, M., 2013. Amaryllidaceae alkaloids inhibit nuclear-to-cytoplasmic export of ribonucleoprotein (RNP) complex of highly pathogenic avian influenza virus H5N1. Influenza Other Respir. Viruses 7, 922–931.

Hu, Y., Sneyd, H., Dekant, R., Wang, J., 2017. Influenza A virus nucleoprotein: a highly conserved multi-functional viral protein as a hot antiviral drug target. Curr. Top. Med. Chem. 17, 2271–2285.

Jalily, P.H., Duncan, M.C., Fedida, D., Wang, J., Tietjen, I., 2020. Put a cork in it: plugging the M2 viral ion channel to sink influenza. Antiviral Res. 178, 104780.

Jang, Y., Lee, H.W., Shin, J.S., Go, Y.Y., Kim, C., Shin, D., Malpani, Y., Han, S.B., Jung, Y.S., Kim, M., 2016. Antiviral activity of KR-23502 targeting nuclear export of influenza B virus ribonucleoproteins. Antiviral Res. 134, 77–88.

Kakisaka, M., Sasaki, Y., Yamada, K., Kondoh, Y., Hikono, H., Osada, H., Tomii, K., Saito, T., Aida, Y., 2015. A novel antiviral target structure involved in the RNA binding, dimerization, and nuclear export functions of the influenza A virus nucleoprotein. PLoS Pathog. 11, e1005062.

Kang, Q., Wang, Y., Cui, Q., Gong, L., Yang, Y., Jiang, H., Rong, L., Rong, R., Du, R., 2020. Screening for anti-influenza actives of prefractionated traditional chinese medicines. Evid Based Complement. Alternat. Med. 2020, 4979850.

Kao, R.Y., Yang, D., Lau, L.S., Tsui, W.H., Hu, L., Dai, J., Chan, M.P., Chan, C.M., Wang, P., Zheng, B.J., Sun, J., Huang, J.D., Madar, J., Chen, G., Chen, H., Guan, Y., Yuen, K.Y., 2010. Identification of influenza A nucleoprotein as an antiviral target. Nat. Biotechnol. 28, 600–605.

Lackenby, A., Besselaar, T.G., Daniels, R.S., Fry, A., Gregory, V., Gubareva, L.V., Huang, W., Hurt, A.C., Leang, S.K., Lee, R.T.C., Lo, J., Lollis, L., Maurer-Stroh, S., Odagiri, T., Pereyaslov, D., Takashita, E., Wang, D., Zhang, W., Meijer, A., 2018. Global update on the susceptibility of human influenza viruses to neuraminidase inhibitors and status of novel antivirals, 2016-2017. Antiviral Res. 157, 38–46.

Li, T.C., Chan, M.C., Lee, N., 2015. Clinical Implications of antiviral resistance in influenza. Viruses 7, 4929–4944.
Lin, M.I., Su, B.H., Lee, C.H., Wang, S.T., Wu, W.C., Dangate, P., Wang, S.Y., Huang, W.I., Cheng, T.J., Lin, O.A., Cheng, Y.S., Tseng, Y.J., Sun, C.M., 2015. Synthesis and inhibitory effects of novel pyrimido-pyrrolo-quinoxalinedione analogues targeting nucleoproteins of influenza A virus H1N1. Eur. J. Med. Chem. 102, 477–486.
Lin, X., Zhu, M., Zhao, X., Si, L., Dong, M., Anirudhan, V., Cui, Q., Rong, L., Du, R., 2023. Optimization and applications of an in vivo bioluminescence imaging model of influenza A virus infections. Virol. Sin. 38, 631–634.
Liu, C.L., Hung, H.C., Lo, S.C., Chiang, C.H., Chen, I.J., Hsu, J.T., Hou, M.H., 2016. Using mutagenesis to explore conserved residues in the RNA-binding groove of influenza A virus nucleoprotein for antiviral drug development. Sci. Rep. 6, 21662.
Makau, J.N., Watanabe, K., Otaki, H., Mizuta, S., Ishikawa, T., Kamatari, Y.O., Nishida, N., 2020. A Quinolinone compound inhibiting the oligomerization of nucleoprotein of influenza A virus prevents the selection of escape mutants. Viruses 12, 337.
Martin, K., Helenius, A., 1991. Nuclear transport of influenza virus ribonucleoproteins: the viral matrix protein (M1) promotes export and inhibits import. Cell 67, 117–130.
Morris, G.M., Huey, R., Lindstrom, W., Sanner, M.F., Belew, R.K., Goodsell, D.S., Olson, A.J., 2009. AutoDock4 and AutoDockTools4: automated docking with selective receptor flexibility. J. Comput. Chem. 30, 2785–2791.
Newcomb, L.L., Kuo, R.L., Ye, Q., Jiang, Y., Tao, Y.J., Krug, R.M., 2009. Interaction of the influenza a virus nucleocapsid protein with the viral RNA polymerase potentiates unprimed viral RNA replication. J. Virol. 83, 29–36.
Noshi, T., Kitano, M., Taniguchi, K., Yamamoto, A., Omoto, S., Baba, K., Hashimoto, T., Ishida, K., Kushima, Y., Hattori, K., Kawai, M., Yoshida, R., Kobayashi, M., Yoshinaga, T., Sato, A., Okamatsu, M., Sakoda, Y., Kida, H., Shishido, T., Naito, A., 2018. In vitro characterization of baloxavir acid, a first-in-class cap-dependent endonuclease inhibitor of the influenza virus polymerase PA subunit. Antiviral Res. 160, 109–117.
Noton, S.L., Medcalf, E., Fisher, D., Mullin, A.E., Elton, D., Digard, P., 2007. Identification of the domains of the influenza A virus M1 matrix protein required for NP binding, oligomerization and incorporation into virions. J. Gen. Virol. 88, 2280–2290.
Pang, B., Cheung, N.N., Zhang, W., Dai, J., Kao, R.Y., Zhang, H., Hao, Q., 2016. Structural characterization of H1N1 nucleoprotein-nucleozin binding sites. Sci. Rep. 6, 29684.
Perwitasari, O., Johnson, S., Yan, X., Howerth, E., Shacham, S., Landesman, Y., Baloglu, E., McCauley, D., Tamir, S., Tompkins, S.M., Tripp, R.A., 2014. Verdinexor, a novel selective inhibitor of nuclear export, reduces influenza a virus replication in vitro and in vivo. J. Virol. 88, 10228–10243.
Poland, G.A., 2010. The 2009-2010 influenza pandemic: effects on pandemic and seasonal vaccine uptake and lessons learned for seasonal vaccination campaigns. Vaccine 28 (Suppl 4), D3–13.
Sherry, L., Smith, M., Davidson, S., Jackson, D., 2014. The N terminus of the influenza B virus nucleoprotein is essential for virus viability, nuclear localization, and optimal transcription and replication of the viral genome. J. Virol. 88, 12326–12338.
Shiraki, K., Daikoku, T., 2020. Favipiravir, an anti-influenza drug against life-threatening RNA virus infections. Pharmacol. Ther. 209, 107512.
Takashita, E., Ichikawa, M., Morita, H., Ogawa, R., Fujisaki, S., Shirakura, M., Miura, H., Nakamura, K., Kishida, N., Kuwahara, T., Sugawara, H., Sato, A., Akimoto, M., Mitamura, K., Abe, T., Yamazaki, M., Watanabe, S., Hasegawa, H., Odagiri, T., 2019. Human-to-human transmission of influenza A(H3N2) virus with reduced susceptibility to baloxavir, Japan, February 2019. Emerg. Infect. Dis. 25, 2108–2111.
Taubenberger, J.K., Kash, J.C., 2010. Influenza virus evolution, host adaptation, and pandemic formation. Cell Host Microbe 7, 440–451.
Tscherne, D.M., Garcia-Sastre, A., 2011. Virulence determinants of pandemic influenza viruses. J. Clin. Invest. 121, 6–13.
Turrell, L., Lyall, J.W., Tiley, L.S., Fodor, E., Vreede, F.T., 2013. The role and assembly mechanism of nucleoprotein in influenza A virus ribonucleoprotein complexes. Nat. Commun. 4, 1591.
van der Vries, E., Schutten, M., Fraaij, P., Boucher, C., Osterhaus, A., 2013. Influenza virus resistance to antiviral therapy. Adv. Pharmacol. 67, 217–246.
Wang, Z., Zhao, F., Gao, Q., Liu, Z., Zhang, Y., Li, X., Li, Y., Ma, W., Deng, T., Zhang, Z., Cen, S., 2015. Establishment of a high-throughput assay to monitor influenza A virus RNA transcription and replication. PLoS One 10, e0133558.
White, K.M., Abreu Jr., P., Wang, H., De Jesus, P.D., Manicassamy, B., García-Sastre, A., Chanda, S.K., DeVita, R.J., Shaw, M.L., 2018. Broad spectrum inhibitor of influenza A and B viruses targeting the viral nucleoprotein. ACS Infect. Dis. 4, 146–157.
Yang, F., Pang, B., Lai, K.K., Cheung, N.N., Dai, J., Zhang, W., Zhang, J., Chan, K.H., Chen, H., Sze, K.H., Zhang, H., Hao, Q., Yang, D., Yuen, K.Y., Kao, R.Y., 2021. Discovery of a novel specific inhibitor targeting influenza A virus nucleoprotein with pleiotropic inhibitory effects on various steps of the viral life cycle. J. Virol. 95, e01432–20.
Yu, M., Liu, X., Cao, S., Zhao, Z., Zhang, K., Xie, Q., Chen, C., Gao, S., Bi, Y., Sun, L., Ye, X., Gao, G.F., Liu, W., 2012. Identification and characterization of three novel nuclear export signals in the influenza A virus nucleoprotein. J. Virol. 86, 4970–4980.
Zhang, J., Huang, F., Tan, L., Bai, C., Chen, B., Liu, J., Liang, J., Liu, C., Zhang, S., Lu, G., Chen, Y., Zhang, H., 2016. Host protein moloney leukemia virus 10 (MOV10) acts as a restriction factor of influenza A virus by inhibiting the nuclear import of the viral nucleoprotein. J. Virol. 90, 3966–3980.
Zhang, Y., Xu, W.F., Yu, Y., Zhang, Q., Huang, L., Hao, C., Shao, C.L., Wang, W., 2023. Inhibition of influenza A virus replication by a marine derived quinolone alkaloid targeting virus nucleoprotein. J. Med. Virol. 95, e28499.
Zhao, X., Wang, Y., Cui, Q., Li, P., Wang, L., Chen, Z., Rong, L., Du, R., 2019. A parallel phenotypic versus target-based screening strategy for RNA-dependent RNA polymerase inhibitors of the influenza A virus. Viruses 11, 826.
Zhao, X., Wang, L., Cui, Q., Li, P., Wang, Y., Zhang, Y., Yang, Y., Rong, L., Du, R., 2018. A mechanism underlying attenuation of recombinant influenza A viruses carrying reporter genes. Viruses 10, 679.
Zhao, X., Lin, X., Li, P., Chen, Z., Zhang, C., Manicassamy, B., Rong, L., Cui, Q., Du, R., 2022. Expanding the tolerance of segmented influenza A Virus genome using a balance compensation strategy. PLoS Pathog. 18, e1010756.
Zheng, W., Fan, W., Zhang, S., Jiao, P., Shang, Y., Cui, L., Mahesutihan, M., Li, J., Wang, D., Gao, G.F., Sun, L., Liu, W., 2019. Naproxen exhibits broad anti-influenza virus activity in mice by impeding viral nucleoprotein nuclear export. Cell Rep. 27, 1875–1885 e1875.